Journal of Hydrology 556 (2018) 1192–1204

Contents lists available at ScienceDirect

Journal of Hydrology

journal homepage: www.elsevier.com/locate/jhydrol

Research papers

Estimation of the climate change impact on a catchment water balance using an ensemble of GCMs

T.V. Reshmidevi [a], D. Nagesh Kumar [b,c,*], R. Mehrotra [d], A. Sharma [d]

[a] Department of Civil Engineering, BMS College of Engineering, Bangalore 560019, India
[b] Department of Civil Engineering, Indian Institute of Science, Bangalore 560012, India
[c] Divecha Centre for Climate Change, Indian Institute of Science, Bangalore 560012, India
[d] Water Research Centre, School of Civil and Environmental Engineering, UNSW, 2052 Sydney, Australia

ARTICLE INFO

Article history:
Available online 14 February 2017

Keywords:
ArcSWAT
GCM
Climate change
MMM-KDE downscaling model

ABSTRACT

This work evaluates the impact of climate change on the water balance of a catchment in India. Rainfall and hydro-meteorological variables for current (20C3M scenario, 1981–2000) and two future time periods: mid of the 21st century (2046–2065) and end of the century (2081–2100) are simulated using Modified Markov Model-Kernel Density Estimation (MMM-KDE) and k-nearest neighbor downscaling models. Climate projections from an ensemble of 5 GCMs (MPI-ECHAM5, BCCR-BCM2.0, CSIRO-mk3.5, IPSL-CM4, and MRI-CGCM2) are used in this study. Hydrologic simulations for the current as well as future climate scenarios are carried out using Soil and Water Assessment Tool (SWAT) integrated with ArcGIS (ArcSWAT v.2009). The results show marginal reduction in runoff ratio, annual streamflow and groundwater recharge towards the end of the century. Increased temperature and evapotranspiration project an increase in the irrigation demand towards the end of the century. Rainfall projections for the future shows marginal increase in the annual average rainfall. Short and moderate wet spells are projected to decrease, whereas short and moderate dry spells are projected to increase in the future. Projected reduction in streamflow and groundwater recharge along with the increase in irrigation demand is likely to aggravate the water stress in the region under the future scenario.

1. Introduction

Global climate change and its impact on hydrologic processes have been widely discussed in the recent past. With increase in temperature, climate change is accelerating the global hydrologic cycle (Huntington, 2006; Oki and Kanae, 2006). Climate change is projected to cause changes in precipitation pattern, variation in the frequency and distribution of floods and droughts, and increase in evapotranspiration rate over different regions in the world (Frederick and Major, 1997; Ficklin et al., 2012). Under the changing climate scenario, changes in streamflows have been found to be largely linked with the variations in precipitation. However for some locations, especially for moisture limited regions, small increase in temperature and the associated increase in evapotranspiration can cause larger variations in streamflows (McCabe and Wolock, 2011). In a study by Sankarasubramanian and Vogel (2003), storage processes within the catchment have been identified as the major factor that defines the non-linearity between the streamflow and precipitation. For moisture limited arid regions, actual evapotranspiration is limited due to the limited moisture availability. For such regions, any increase in precipitation causes a proportional increase in actual evapotranspiration, causing changes in the runoff to be less dramatic. On the other hand in humid regions, where moisture availability is not limited, any increase in precipitation may not result in proportional increase in evapotranspiration. In other words, changes in evapotranspiration rate with respect to changes in rainfall are less prominent. Therefore, any changes in rainfall are likely to cause larger changes in streamflow (Sankarasubramanian and Vogel, 2003). Basin level hydrologic analyses are therefore essential to assess the sensitivity of the basin to climate change scenarios, and to develop appropriate water resources management policies and climate change adaptation strategies.

Global Climate Models (GCMs) are the primary tools that provide future projections of climate variables in the changing environment. GCMs are complex mathematical models capable of simulating the behavior of the Earth's atmosphere, ocean and land surface in three dimensions (McGuffie and Henderson-Sellers,

* Corresponding author at: Department of Civil Engineering, Indian Institute of Science, Bangalore 560012, India.
E-mail address: nagesh@civil.iisc.ernet.in (D. Nagesh Kumar).

http://dx.doi.org/10.1016/j.jhydrol.2017.02.016
0022-1694/

1997). However, they remain relatively coarse in resolution, and are unable to resolve significant sub-grid scale features often necessary in any hydrologic study (Allen and Ingram, 2002; Fowler et al., 2007). Therefore, studies dealing with the climate change impact assessment at catchment scale require downscaling of GCM projections to an appropriate scale to represent the catchment heterogeneity (Silberstein et al., 2012). Various statistical (Anandhi et al., 2008; Mehrotra and Sharma, 2010) and dynamic downscaling methods (Misra et al., 2003; Dominguez et al., 2012) have been adopted in the past to downscale large scale atmospheric variables from the GCMs to a regional scale or to a finer scale representative of a catchment.

Downscaled climate simulations are often used as an input to hydrologic models to simulate the hydrologic responses and to assess the impact of climate change on water resources (Chang and Jung, 2010; Vaze and Teng, 2011; Ruelland et al., 2012). In such studies the hydrologic models are first calibrated using historic data, and then run using future scenarios to translate the climate change signals into corresponding changes in the hydrologic responses. When GCM data are used, large amount of uncertainty is inherent in the analyses. For instance, climate change projections are based on the Green House Gas (GHG) emission scenarios under different conditions of economic and technological development, as well as the balance between global and local growth. There are many emission scenarios mentioned in the Special Report on the Emission Scenario-SRES (IPCC, SRES, 2000). Besides that, there are many GCMs available, giving different projections of the climate variables for the same future GHG emission scenario. From the previous studies (Wilby and Harris, 2006; Chen et al., 2011), choice of a single GCM has been consistently identified as the major contributor to the overall uncertainty in such analyses. Uncertainties arising from GHG emission scenario and the hydrologic model structure have been identified to be the least significant (Wilby and Harris, 2006; Minville et al., 2008; Chen et al., 2011; Woldemeskel et al., 2012). Due to the large uncertainty introduced by the GCMs, climate change impacts estimated from the use of a single GCM need to be interpreted cautiously. Hence, multi-model ensemble climate simulations have been used in many of the recent studies (Tebaldi and Knutti, 2007; Knutti et al., 2010; Jung et al., 2012; Zhang and Huang, 2013). Multi-model mean has been found to be giving better simulation of the climate variables compared to the individual models (Gleckler et al., 2008; Knutti et al., 2010; Zhang and Huang, 2013).

In light of these facts, in this study, the hydrologic impact of climate change on Malaprabha catchment in India is evaluated using climate projections from an ensemble of 5 GCMs. Rainfall and meteorological variables are downscaled from large scale atmospheric variables simulated by the GCMs. A conceptual, yet spatially distributed hydrologic model SWAT is used to derive the hydrologic simulation using inputs from each GCM. In this study, SWAT integrated with ArcGIS graphical user interface (ArcSWAT. V. 2009) is adopted. A weighted ensemble average approach is used to estimate the average hydrologic responses of the catchment under future scenarios and to evaluate the hydrologic impact of climate change in the catchment.

The World Climate Research Programme's Coupled Model Intercomparison Project phase 3 (CMIP3) and CMIP5 datasets each contain output from a large number of GCMs. Both datasets use different scenarios describing the amount of greenhouse gas in the atmosphere in the future. CMIP3 uses scenarios from the Intergovernmental Panel on Climate Change's (IPCC) Special Report on Emissions Scenarios (SRES) whereas CMIP5 uses Representative Concentration Pathways recommended in the IPCC Fifth Assessment Report (IPCC, 2013). In this study, GCMs included in the CMIP3 project and IPCC SRES emission scenario are used to obtain the climate projection for the 20th century as well as the future scenarios. The IPCC notes that, for both large-scale climate patterns and the magnitudes of climate change, there is overall consistency between the projections based on CMIP3 and CMIP5 (IPCC, 2013). Results of a few recent studies show that both CMIP3 and CMIP5 models well simulate the large scale atmospheric variables used in this study for the statistical downscaling of rainfall (Mueller and Seneviratne, 2014; Woldemeskel et al., 2016). In addition, based on the studies conducted using CMIP3 and CMIP5 models, Shashikanth et al. (2014) concluded that the Indian Summer Monsoon Rainfall simulations from both models do not differ significantly. Hence the current study helps to understand the sensitivity of the catchment to the projected climate scenarios, even though an additional analysis using CMIP5 models and appropriate RCPs would further strengthen the findings of the study.

2. Study area and input data

2.1. Study area

Malaprabha River originates from the Western Ghats in the Belgaum District in North Karnataka, India. The area drained by Malaprabha River and its tributaries up to Malaprabha dam is selected as the present study area. The catchment area is 2564 sq.km with elevation ranging from 1024 m to 430 m. Location map of the Malaprabha catchment is shown in Fig. 1, based on the Survey of India maps (http://www.surveyofindia.gov.in/).

Climatology of the catchment varies from tropical humid in the upper catchment to semi arid in the lower catchment. Annual average rainfall in the catchment exhibits large spatial variation ranging from 3000 mm in the upper region to less than 500 mm in the lower region. Annual average rainfall, averaged over the catchment is 1051 mm, much of which is received during the south-west monsoon period from June to September (Anandhi et al., 2008). Mean monthly maximum and minimum temperatures in the catchment vary from 25 to 34 °C and 17 to 21 °C, respectively (Anandhi et al., 2009). Malaprabha reservoir is the major source of irrigation water for the 218,191 hectares (Anandhi et al., 2009) of agricultural area in the arid regions in north Karnataka, and is also the major source of drinking water for about one million people in Hubli and Dharwad cities. Malaprabha catchment is a hydrologically sensitive area such that any change in water yield in the catchment is likely to effect vast areas that are dependent on the reservoir for irrigation and drinking water. In addition, due to extensive groundwater extraction to meet the irrigation demand, groundwater table in a large part of the catchment has been drastically depleted (CGWB, 2007; Reshmidevi and Nagesh Kumar, 2012). Scientific studies are therefore essential to analyse the hydrologic responses of this water scarce catchment under the projected climate change scenario to facilitate the planning of appropriate mitigation measures.

2.2. Data used

Digital elevation model (DEM), digital soil map and land use/land cover (LU/LC) map are used to represent the catchment heterogeneity for the hydrologic analysis. DEM of Malaprabha catchment at 30 m spatial resolution is obtained from Advanced Space-borne Thermal Emission and Reflection Radiometer (ASTER) Global DEM (GDEM) data set released by the Japan's Ministry of Economy, Trade and Industry (METI) and NASA. Multi season Landsat-7 ETM+ imageries are used to extract LU/LC map of the catchment. In this study, a combination of visual and digital image interpretation technique is used to extract the LU/LC map from the satellite imagery (Reshmidevi and Nagesh Kumar, 2012). Seven main LU/LC classes viz., water, agricultural land, barren/fallow

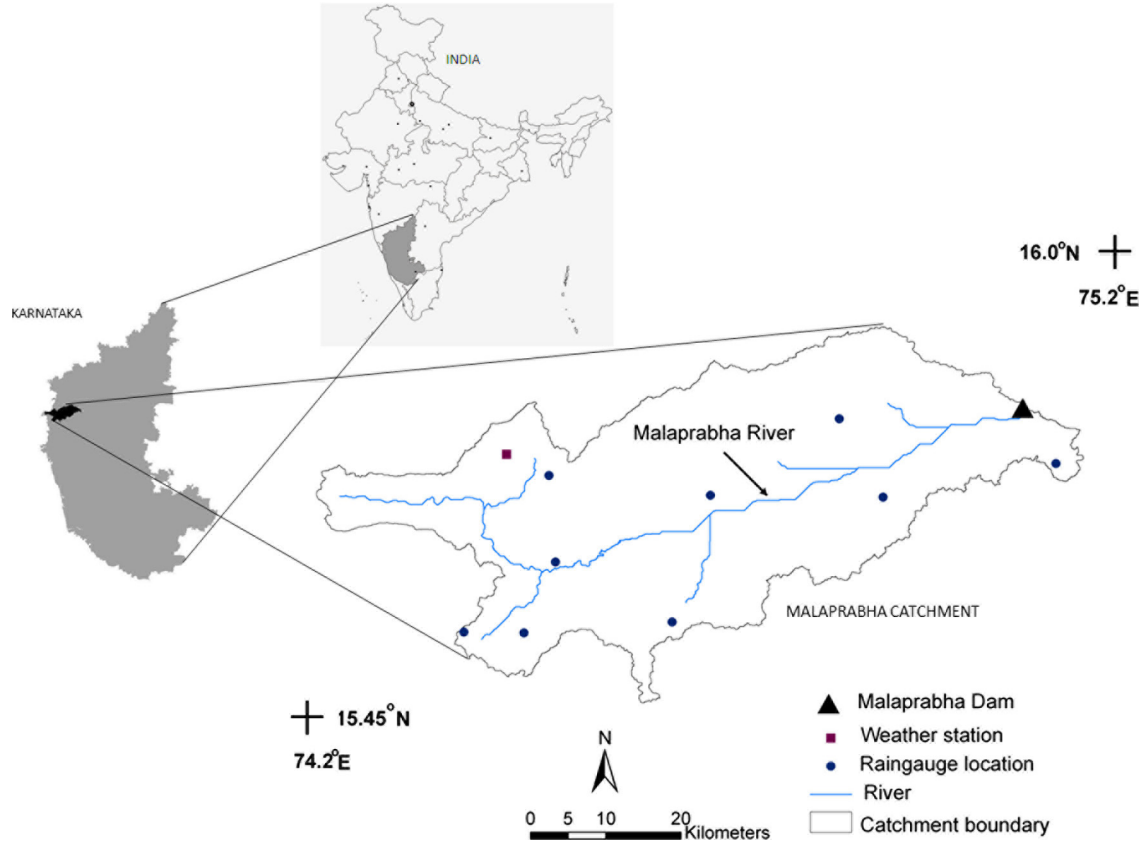

Fig. 1. Location map of the Malaprabha catchment.

land, rocky area, forest, urban settlement and grass land are extracted in the first step. Appropriate bands that show unique band ratio are identified for each land cover class. A combination of visual interpretation and unsupervised classification using band ratio (Lillesand et al., 2004) is used to identify the seven major land cover classes. The second level classification, i.e., classification of the crop types is achieved using multi-temporal satellite images (Dutta et al., 1998) representing different cropping seasons. Depending upon the presence or absence of crop in each image, different crop types are classified. Field information and the district statistical information about the crop production are used to substantiate the classification.

Soil map of the area is obtained from the National Bureau of Soil Survey and Land Use Planning, Nagpur, India. Monthly inflow into the Malaprabha reservoir for the period 1973–2000 is obtained from the Water Resources Development Organization, Bangalore, India and is used as the observed streamflow data to calibrate the hydrologic model.

Rainfall and meteorological variables viz., maximum and minimum temperatures and relative humidity at daily time steps are used for hydrologic simulation. In order to incorporate the large spatial heterogeneity, rainfall data from 9 stations are used in this study. Locations of the stations for which the downscaled rainfall and meteorological data are available are shown in Fig. 1. Daily rainfall data at these 9 stations in the catchment are available for the period 1971–2000, whereas observed meteorological data are available only for a short period 1993–2000. Mass curve analysis of the rainfall data was performed, from which the period 1993–2000 was found to be insufficient to represent the entire study period 1971–2000. Therefore, rainfall and meteorological variables are downscaled from the National Centre for Environmental Prediction (NCEP) reanalysis data for the period 1971–2000. In addition, for historic and future time periods, rainfall and hydrometeorological variables are downscaled from multiple GCMs. Modified Markov Model-Kernel Density Estimation (MMM-KDE) model (Mehrotra and Sharma, 2010) is used to downscale rainfall from large scale atmospheric variables to the multiple raingauge stations shown in Fig. 1. Also, the k-nearest neighbor resampling method is used to downscale the meteorological variables to the single location shown in Fig. 1. The MMM-KDE model and the k-nearest neighbor resampling methods are explained in the next section.

Based on the easy availability of daily data of the atmospheric variables from the World Climate Research Programme's Coupled Model Intercomparison Project phase 3 (CMIP3), 5 GCMs are considered in this study. These are (i) BCCR-BCM2.0 developed by the Bjerknes Centre for Climate Research (BCCR), University of Bergen, Norway, (ii) MRI-CGCM2 developed by the Meteorological Research Institute (MRI), Japan, (iii) CSIRO-mk3.5 developed by the Commonwealth Scientific and Industrial Research Organization (CSIRO), Australia, (iv) MPI-ECHAM5 developed by the Max Planck Institute for Meteorology (MPI), Germany, and (v) IPSL-CM4 developed by the Institute Pierre Simon Laplace (IPSL), France. The 20th century climate experiment (20C3M) for the period 1981–2000 is selected to represent the historic scenario. Hydrologic impact of climate change is also studied for two 20 year future time periods: 2046–2065 (referred hereafter as mid of the century) to represent the mid 21st century, and 2081–2100 (referred hereafter as end of the century) to represent the end of 21st century. For each time period, required atmospheric variables at GCM grid nodes over the catchment are extracted from a single continuous (transient) run corresponding to SRES A2 emission scenario. The A2 scenario, which is at the higher end of the SRES emission scenarios (but not the highest), is selected in this study as it would be more informa-

tive from impact and adaptation point of view compared to the lower end scenario. Hydrologic model SWAT is used to simulate the catchment hydrologic responses for historic and two future time periods under the A2 scenario. Please note that during the time of this study, runs from the Coupled Model Intercomparison Project phase 5 (CMIP5) were not available. Nevertheless, many studies have raised concerns about whether CMIP5 models are capturing the historic monsoon trends accurately (Kitoh et al., 2013; Ogata et al., 2014; Sooraj et al., 2014; Saha et al., 2014) and whether the monsoon projections are reliable in these models (Sabeerali et al., 2014). Recent study by Shashikanth et al. (2014) shows that biases in the statistically downscaled Indian Summer Monsoon Rainfall (ISMR) data do not differ significantly for CMIP3 and CMIP5 data sets. In this study, future estimates of runoff and rainfall are derived using smooth varying atmospheric variables which are considered to be equally well estimated by majority of GCMs used in both CMIP3 and CMIP5 projects (Mueller and Seneviratne, 2014; Woldemeskel et al., 2016). Hence the current study is restricted only to the CMIP3 data.

3. Methodology and model description

3.1. Statistical downscaling of rainfall and meteorological variables

The variable convergence score (Johnson and Sharma, 2009) is used to identify the GCM atmospheric variables for use in downscaling daily rainfall. These variables include mean sea level pressure (MSLP), north-south (N-S) gradient of MSLP, temperature depressions (TD) at 850 hPa, 700 hPa, 500 hPa, N-S gradient of TD at 850 hPa, U and V components of the wind velocities at 850 hPa, Equivalent potential temperature (EPT) at 850 hPa, N-S gradient of the geopotential height (GPH) at 700 hPa, specific humidity (SPH) at 500 hPa, N-S gradient of SPH at 500 hPa and E-W gradient of SPH at 850 hPa (Mehrotra et al., 2013). The selected GCM atmospheric variables for 20C3M (1981–2000) and future time periods (2046-65 and 2081-2100) are then bias-corrected by adopting a nested bias correction procedure (Johnson and Sharma, 2012). The nested bias correction (NBC) method offers an improvement over the quantile mapping method by incorporating the persistence of rainfall through lag-1 autocorrelation. Also, corrections are nested from finer to coarser time scales, by which the GCM outputs are corrected for biases in mean, standard deviation and Lag-1 auto-correlation at daily, monthly, seasonal and annual time scales simultaneously. Any biases in the GCM atmospheric fields are thus removed before their use for downscaling, while the mean shift from current to future climate is preserved. Previous studies have demonstrated successful use of NBC for bias correction of atmospheric variables in reproducing the observed low frequency variability in the rainfall simulations (Johnson and Sharma, 2011; Sharma et al., 2012; Ojha et al., 2013).

Modified Markov Model-Kernel Density Estimation (MMM-KDE) modelling framework (Mehrotra and Sharma, 2010) is used to downscale rainfall at multiple sites in the catchment. The model operates in two steps: in the first step the Modified Markov Model (MMM) is used to identify wet and dry days, and in the second step intensity of rainfall during wet days is estimated using the Kernel Density Estimation (KDE) approach. A wet day is defined as a day with rainfall greater than or equal to 0.3 mm.

Markov model is a stochastic model that predicts a state variable at any point of time as a function of the variable in the previous time step. In MMM, to include the influence of changing climate, the simple Markov model is modified by including atmospheric predictors as conditioning variables. Thus in MMM, probability of occurrence of a wet or dry day consists of two terms, first term showing the transition probability of rainfall similar to a simple Markov model and the second term showing the effect of inclusion of a predictor set consisting of the atmospheric variables of interest. The KDE approach simulates the intensity of rainfall during each time step (which is identified as a wet day by the MMM) based on the rainfall intensity of previous time step and selected atmospheric variables. Conditional nonparametric multivariate probability density of rainfall amount R_t for day t for each site may be defined as follows (Mehrotra et al., 2013).

$$f(R_t|\mathbf{X}_t) = \sum_{i=1}^{N} \frac{1}{(2\pi\lambda^2 S')^{1/2}} w_i \exp\left(-\frac{(R_i - b_i)^2}{2\lambda^2 S'}\right) \quad (1)$$

where, λ is the kernel bandwidth and X_t is the vector representing the climate variables influencing the rainfall. S' is the measure of spread of the conditional density, and b_i is the conditional mean, both expressed in terms of covariance between R and X. w_i is the weight associated with each kernel.

Since rainfall at multiple stations are considered in this study, spatial dependence over these point locations at each time step is incorporated by using uniform random variates that are independent in time, but exhibit a strong dependence across the multiple point locations considered. More details on the MMM-KDE model structure are available in Mehrotra and Sharma (2010) and Mehrotra et al. (2013). MMM-KDE model produces multiple realizations of the downscaled variables. In this study, 20 such realizations generated for 20C3M and the future scenarios are considered and the average hydrologic responses are estimated for each scenario. Daily values of maximum and minimum temperature, and relative humidity are downscaled from the large scale atmospheric variables using the k-nearest neighbor resampling.

3.2. ArcSWAT

ArcSWAT is the Soil and Water Assessment Tool (SWAT), with a powerful user interface integrated with the ArcGIS platform (Winchell et al., 2007). SWAT is a conceptual model capable of simulating the catchment hydrologic processes at a continuous time scale (Arnold et al., 1998). Capability of SWAT to simulate basin level hydrologic characteristics for varying land use and climate conditions makes it a widely adopted tool for climate change studies related to hydrology (Wang et al., 2008; Bae et al., 2011; Ficklin et al., 2012). Geographical Information System (GIS) interface of ArcSWAT allows the users to provide spatially referenced data. Using the topographical information, ArcSWAT divides the catchment into sub-basins. Each sub basin is further divided into homogeneous Hydrological Response Units (HRUs) using the spatially distributed soil, land use/land cover and slope information. Each HRU is vertically divided into different control volumes like surface layer, root zone, shallow aquifer and deep aquifer.

Different approaches and approximations are used to partition the precipitation into various hydrologic components in these control volumes. A part of the precipitation is available as surface runoff and the remaining portion infiltrates into the soil layer. Partitioning of rainfall into surface runoff and infiltration is achieved using the Soil Conservation Services Curve Number (SCS-CN) method (SCS, 1972) embedded in ArcSWAT. Large number of studies conducted over a wide range of catchments have shown that SWAT gives reasonably good simulation of the surface runoff processes (Steenhuis et al., 1995; Ponce and Hawkins, 1996; Mishra and Singh, 2004; Reshmidevi et al., 2008). Runoff from each HRU is further routed through channels to the watershed outlet using the variable storage method (Williams, 1969). A part of infiltrated water leaves the soil layer as lateral flow, which is estimated using a kinematic flow equation involving saturated hydraulic conductivity of the soil layer, slope, drainable porosity and drainable volume of water present in the layer. Another fraction of water that

reaches the soil layer percolates further and joins the groundwater storage, which is called groundwater recharge. Groundwater recharge is computed as a function of drainable volume of water present in the soil layer. This groundwater recharge may be further divided into shallow aquifer recharge and deep aquifer recharge (Reshmidevi and Nagesh Kumar, 2012). Shallow aquifer storage contributes to the groundwater flow and adds to the streamflow within the watershed, whereas groundwater flow from the deep aquifer is assumed to meet the stream only outside the catchment.

In this study, Hargreaves method (Hargreaves and Samani, 1985) available in the ArcSWAT interface is used for estimating potential evapotranspiration (PET). ArcSWAT provides options to define various agricultural operations for each crop at the HRU level. Irrigation requirement for the crops is defined according to the plant water stress condition (Reshmidevi and Nagesh Kumar, 2012). Digital elevation model of the catchment, spatial variation in soil and LU/LC are the primary spatially referenced data used in ArcSWAT. Rainfall and meteorological data viz., maximum and minimum temperature, and relative humidity at daily time step are also used as input to the model. Details of ArcSWAT components can be found in literature (Arnold et al., 1998).

3.3. ArcSWAT calibration and validation

ArcSWAT (v.2009) is applied at daily time scale over the study area. The catchment is first divided into 12 sub-basins and each sub-basin is further divided into HRUs using the LU/LC, soil and slope information. Irrigated areas in the catchment are identified and the irrigation application is defined when plant water stress exceeds a threshold of 0.95. Daily values of rainfall at 9 stations and hydro-meteorological variables at the single location shown in Fig. 1, are downscaled from the reanalysis data and are used for model calibration and validation. Simulated discharge is compared with the observed monthly streamflow data. The period 1971–2000 is selected in this study, out of which the first two years are used as the warm-up period for the model and the period 1973–2000 is used for model calibration and validation. Multiple realizations of the downscaled rainfall and climate variables produced by MMM-KDE approach are used in the hydrologic modelling. In order to derive stable values of model parameters during calibration, concatenated data set is formed using multiple realizations. From the ensemble of 20 realizations first 9 realizations are used for calibration and the remaining 11 realizations are used for model validation. Each realization being of 28 years (excluding the warm-up period) total length of the calibration run is thus 252 years.

Model sensitivity analysis is performed using Latin Hypercube (LH) and One-factor-At-a-Time (OAT) methods included in the ArcSWAT (Van Griensven, 2005) and the sensitive parameters are manually calibrated. Capability of the model to accurately produce flow-duration curve (FDC) for the annual and monsoon (June–September) streamflows is considered as the evaluation criteria during calibration. Using monthly streamflow simulations from the model, annual and monsoon streamflows are calculated for each realization and the average FDCs for the annual and monsoon periods are generated. Deviation of the simulated FDC from the observed FDC is measured using mean absolute relative error (MARE) as given in Eq. (2).

$$MARE = \frac{1}{N}\sum_{i=1}^{N}\left|\frac{(Q_{obs} - Q_{sim})}{Q_{sim}}\right| \quad (2)$$

where, N is the number of points considered from the FDC, Q_{obs} and Q_{sim} are the corresponding flow values from the observed FDC and the simulated FDC, respectively.

3.4. Multi-model ensemble projection under the future scenario

Ensemble of simulations from the hydrologic model, obtained by using rainfall and meteorological data from the 5 GCMs is used to evaluate the hydrologic impact of climate change in the catchment by comparing hydrologic responses in the future time periods with that obtained under 20C3M scenario. When the temporal periods do not overlap, FDCs are commonly used for comparing the flow regimes in the hydrologic analyses (Sugawara, 1979; Yu and Yang, 2000; Westerberg et al., 2011). Since the temporal periods of the 20C3M and the future scenarios do not overlap, FDCs of annual and monsoon flows are used here for the comparison.

A weighted ensemble average approach is used to derive ensemble average streamflow simulation from the 5 GCMs. ArcSWAT is run using the downscaled rainfall and meteorological data from each GCM, and FDCs for the annual and monsoon flows are generated. Simulated FDCs for 20C3M scenario are then compared against FDCs of the observed streamflow data for the same period. Deviation of the simulated FDCs from the observed FDC, expressed in terms of MARE is used as the evaluation criterion. For each hydrologic simulation (using input from different GCMs), MARE of the annual and monsoon FDCs are estimated and the mean of these two values is used to derive the weight for each simulation using Eq. (3).

$$weight = \frac{\left(\frac{1}{meanMARE}\right)}{\sum_{m=1}^{5}\left(\frac{1}{meanMARE}\right)} \quad (3)$$

where, m is the model index. Using this set of weights, weighted FDCs of the annual and monsoon flows are generated for the 20C3M scenario and are used as the reference FDCs to quantify the future changes in the streamflow.

GCMs simulating the historic scenario satisfactorily are expected to be capable of simulating the future scenarios reasonably well (Reichler and Kim, 2008; Errasti et al., 2010). Therefore, the weights derived for the hydrologic simulations under 20C3M scenario are adopted for the future time periods as well. Hydrologic responses of the catchment under the future time periods (mid of the century and end of the century), are simulated by using the downscaled rainfall and meteorological variables from each GCM, and the FDCs of both annual and monsoon flows are generated. Further, using the set of weights derived from the 20C3M scenario, weighted average FDCs for the future scenarios are generated. Future projections are compared with 20C3M simulations to quantify the streamflow variation under future scenarios. A flowchart of the methodology is shown in Fig. 2.

Hydrologic simulations from the 5 GCMs are aggregated to find variations in other water budget components viz., potential evapotranspiration (PET), actual evapotranspiration (ET), irrigation demand and groundwater recharge in the future time periods.

3.5. Test for statistical significance

Statistical significance of projected changes in the mean annual and monsoon streamflows is evaluated using non-parametric, rank-based, Mann-Whitney test (Wilcoxon, 1945; Mann and Whitney, 1947). Mann-Whitney test is commonly used to identify statistical significance of the difference in mean or median of hydrological time series (Lettenmaier, 1976; Xu et al., 2003; Caloiero et al., 2011). The test is based on the null hypothesis that medians of the two series compared are the same, and the alternate hypothesis that they differ significantly from one another. When two series of size n_1 and n_2 are compared, the standardized test statistic is represented as follows (Chen et al., 2006).

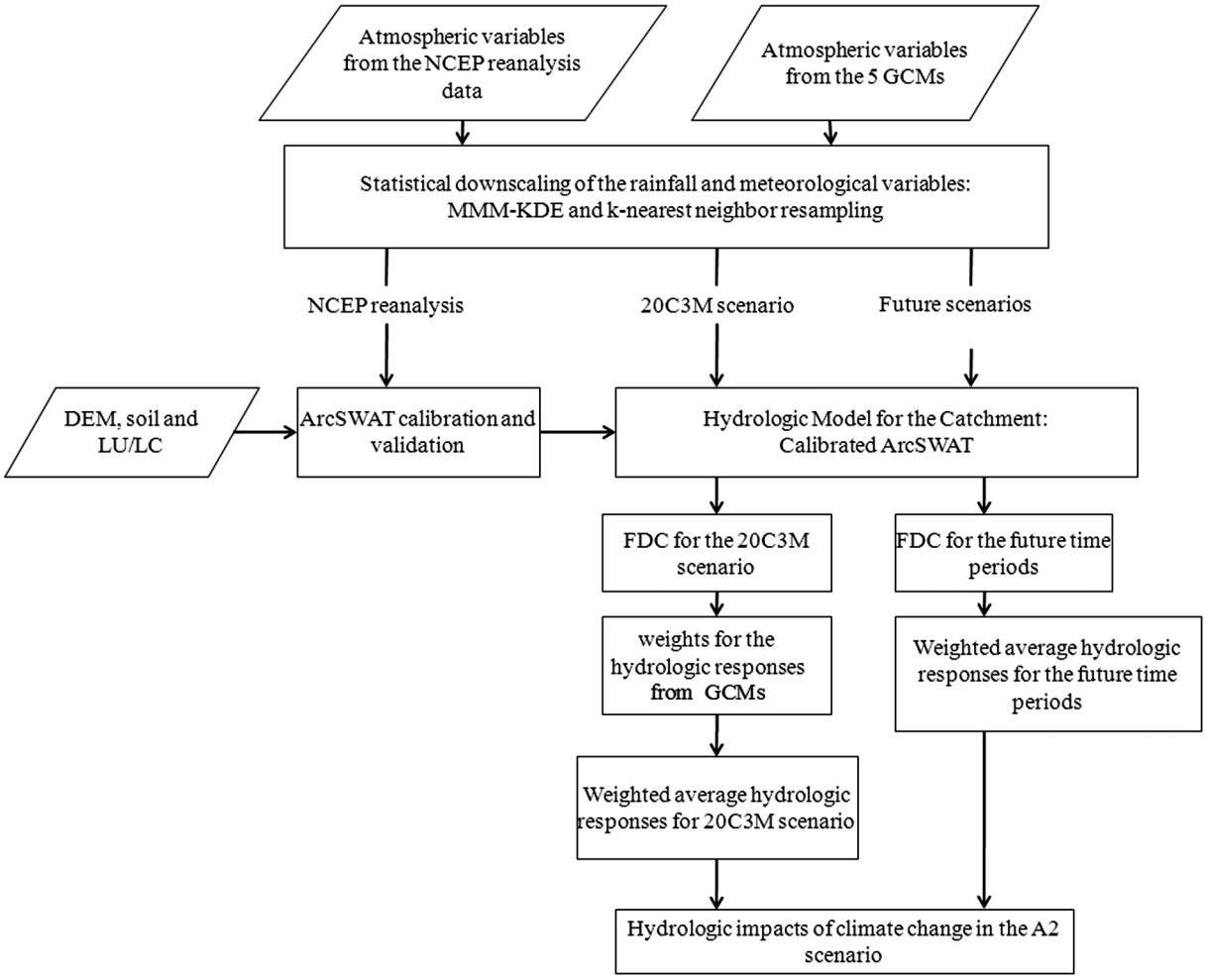

Fig. 2. Schematic representation of the methodology.

$$Z_c = \frac{R_1 - [n_1(n_1 + n_2 + 1)/2]}{\sqrt{n_1 n_2 (n_1 + n_2 + 1)/12}} \quad (4)$$

where, R_1 is the rank sum of the values in series-1. The ranks are assigned by combining all the values in series 1 and 2, and arranging them in the ascending order. For a large sample size the null hypothesis is rejected, in other words a difference between the medians is established, at a significance level α when the probability of occurrence of Z_c obtained from the standardized normal distribution table is greater than or equal to $1 - \alpha/2$.

In this study, the weighted average annual and monsoon streamflow series of the future time periods are compared against the 20C3M scenario and the test statistic is derived. This test statistic is used to find the corresponding α, which indicates the statistical significance of difference in the medians of the two streamflow series compared.

4. Results and discussion

4.1. ArcSWAT calibration and validation

DEM, soil map, and LU/LC map of the Malaprabha catchment are used as spatially referenced input to ArcSWAT to simulate the catchment hydrological processes. The model is run at daily time scale using downscaled rainfall and hydro-meteorological data from the reanalysis data set. Streamflow simulations at daily time scale are aggregated to monthly scale, and are compared with the observed data. Table 1 shows the MARE values for annual and monsoon flows. MARE is found to be less than 0.1 for both calibration and validation phases. Further, monthly streamflow data series is generated taking average of 20 realizations (used for calibration and validation), and the same is compared with the observed monthly streamflow data in Fig. 3. Simulated monthly streamflow series matches well with the observed data, albeit slight underestimation of the peak flow values. Nash-Sutcliffe Efficiency (NSE) coefficient is found to be 0.82, which is considered to be excellent according to the general performance rating for monthly streamflow recommended by Moriasi et al. (2007). Since, a simple averaged monthly flow is used as the benchmark model in NSE, higher values of NSE may be due to the high seasonality of the monthly data. Therefore, as recommended by Schaefli and Gupta (2007), an additional index NSEB is also used in this study to evaluate the model performance. Long-term average streamflow for each month is used as the benchmark model to calculate NSEB. During the calibration period NSEB is obtained as 0.74 for the

Table 1
Performance evaluation index of ArcSWAT in calibration and validation phases.

	MARE	
Phase	Annual	Monsoon
Calibration	0.094	0.072
Validation	0.070	0.084

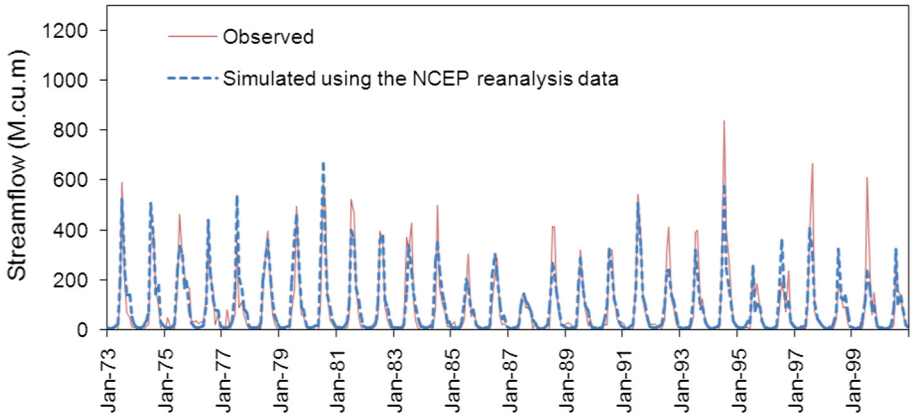

Fig. 3. Comparison of the monthly streamflow hydrograph simulated using the rainfall and meteorological variables downscaled from the NCEP reanalysis data with the observed data.

monthly streamflow simulations. Higher values of NSE and NSEB indicate better performance of the current hydrologic model compared to the selected benchmark models.

The calibrated hydrologic model is used to simulate hydrological responses under 20C3M scenario. Simulated FDCs of annual and monsoon flows obtained using the downscaled rainfall and meteorological data from the 5 GCMs are compared with the FDCs of the observed data in Fig. 4. Table 2 shows the MARE of the annual and monsoon flows for the 5 GCMs and the corresponding weights. Using the set of weights, weighted average FDC for the 20C3M scenario is derived, which is also plotted in Fig. 4. The weighted average annual FDC matches well with the observed data with the exception of some underestimation of moderate and low monsoon flows. This may be mainly due to the small differences between the observed and the downscaled rainfall data in terms of annual wet days and the amount of rainfall per wet day (Mehrotra et al., 2013). Since bias corrected GCM outputs are used in the downscaling, such variations may be due to systemic errors from the downscaling model and therefore, may persist for the future scenarios as well. Hence to quantify the future changes in the streamflow, hydrologic responses in the future time periods are compared with the weighted ensemble average streamflow for the 20C3M scenario.

4.2. Hydrologic responses in the future

Fig. 5 presents the weighted ensemble average FDCs of the annual and monsoon flows for the 20C3M, mid of the century and end of the century scenarios, from which some interesting observations can be drawn. Moderate (corresponding to 40–60% exceedance probability) and high (corresponding to 10% exceedance probability) streamflows at both annual and monsoon timescales show nominal increases for the mid of the century scenario, whereas low flows (corresponding to 90% exceedance probability)

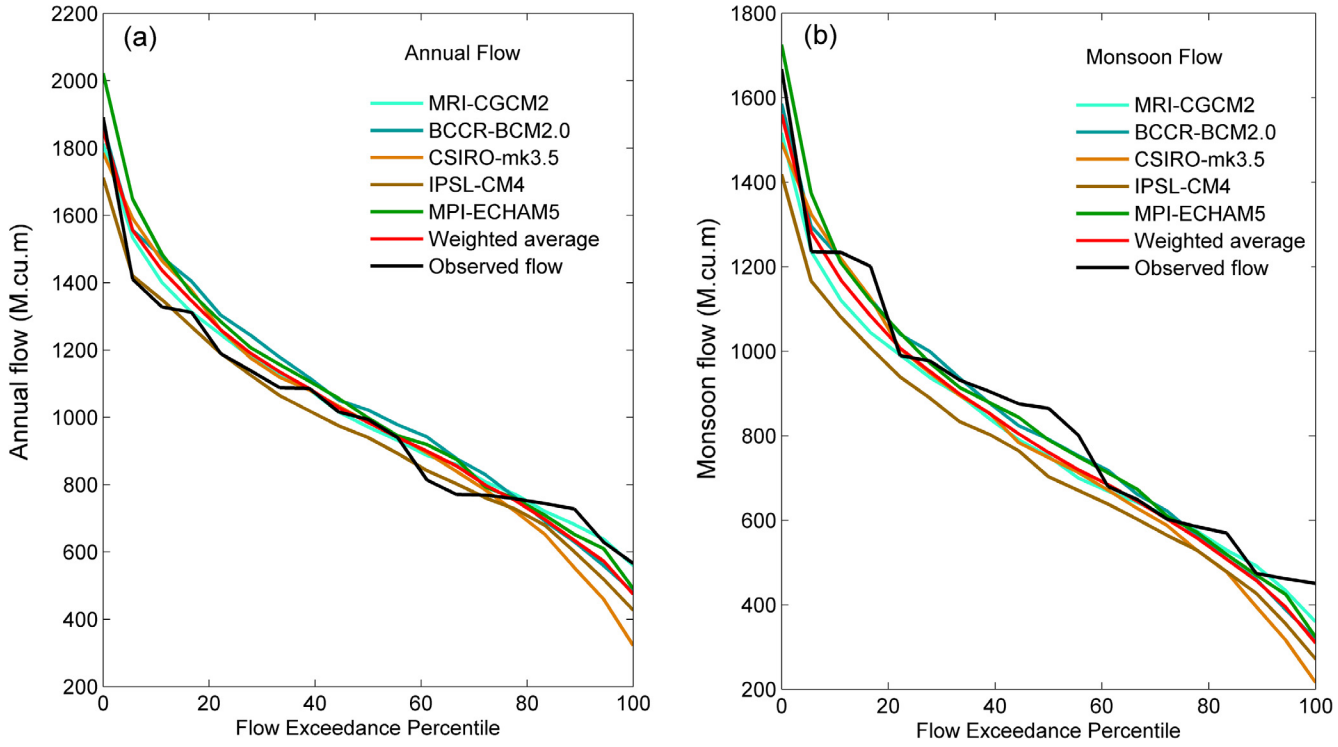

Fig. 4. Simulated Flow-Duration Curves of the annual and monsoon flows for the 20C3M scenario.

Table 2
MARE values of the GCMs for the 20C3M scenario and the corresponding weights.

	MRI-CGCM2	BCCR-BCM2.0	CSIRO-mk3.5	IPSL-CM4	MPI-ECHAM5
Annual MARE	0.039	0.081	0.095	0.063	0.068
Monsoon MARE	0.066	0.064	0.109	0.132	0.058
Weight	0.28	0.20	0.14	0.15	0.23

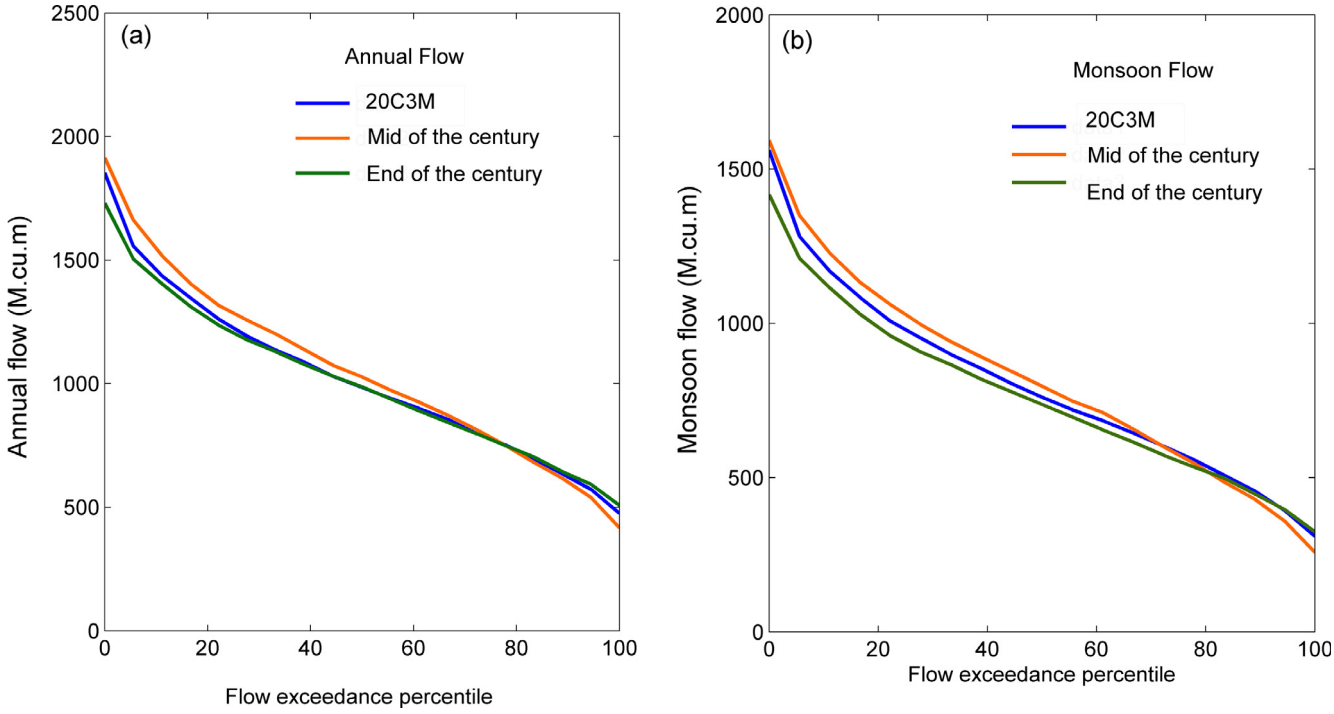

Fig. 5. Weighted ensemble average projections of the annual and monsoon streamflows for the 20C3M, mid of the century and end of the century scenarios.

show some reduction in the future (Fig. 5a and b). Streamflow projections for the end of the century show an overall reduction in monsoon flows as seen from Fig. 5b. This may be attributed to the changes in the rainfall pattern projected towards the end of the century and an increase in the evaporation demand. Study conducted by Mehrotra et al. (2013) shows a plausible reduction in the number of short (2–4 days duration) and moderate (5–7 days duration) wet spells, whereas an increase in the rainfall amounts from short, moderate and long (more than 7 days duration) wet spells over the study area by the mid of the century. On the other hand, short (2–9 days duration) and moderate (10–18 days duration) dry spells are projected to increase under the future scenarios (Mehrotra et al., 2013). Projected increase in the dry spells is likely to cause a reduction in the annual and monsoon low flows.

Using the weighted ensemble simulation, mean annual and monsoon flows are calculated for mid of the century and end of the century scenarios. In addition, annual and monsoon streamflow values corresponding to 10%, 90% and 95% exceedance probability are also estimated from the FDCs, which are given in Table 3. Since streamflow values with less than 10% exceedance probability indicate peak flows, years corresponding to the peak flows are called wet years. On the other hand, 90% and 95% dependable flows indicate lower annual flows, and the years in which annual average flow corresponds to 90% or 95% dependable flows are considered as the low flow years or dry years. The results show an increase in the average annual and monsoon flows in the mid of the century scenario. The study also shows an increase in peak flows as indicated by the increase in the annual and monsoon streamflow values corresponding to 10% exceedance probability. Accordingly, in the mid of the century more number of years are projected to have annual streamflow in excess of the current peak flow corresponding to 10% exceedance probability. In other words, more number of wet years are projected under the mid of the century scenario. Further, a reduction in the 90% and 95% dependable flows indicate an increase in the number of dry years. In other words, frequencies of both wet and dry years are projected to increase towards the mid of the century. Some of the previous studies analyzing the historic rainfall in the 20th century have also reported an increase in the wet and dry years in the changing climate conditions (Changnon, 1987; Sousa et al., 2009).

Streamflow simulations for the end of the century scenario show some reduction in mean annual and monsoon flows corresponding to 10% exceedance probability, whereas no significant changes in the lower flows (90% and 95% dependability). This implies that frequency of wet years is likely to decrease towards the end of the century. These changes, however, are insignificant as indicated by the Mann-Whitney test. The test statistics and significance levels of the percentage changes in the mean annual and monsoon flows are presented in Table 4.

Although, the projected changes in mean annual and monsoon flows are not significant, the intra-annual variation of flows needs to be analysed. Box-whisker plots of the weighted ensemble average monthly flows for the 20C3M and the two future scenarios are shown in Fig. 6. These plots show some variations in the monthly flows during the monsoon period. Median and the

Table 3
Annual and monsoon flow statistics simulated using the 5 GCMs for the 20C3M scenario and the future time periods for the A2 scenario.

		Flow statistics (M.cu.m)*							
		Annual				Monsoon			
GCM	Scenario	1	2	3	4	5	6	7	8
MRI-CGCM2	20C3M	1028.5	1427.2	673.1	630.1	796.6	1143.9	480.4	425.8
	Mid of the century	*1038.1*	*1441.8*	*668.3*	*605.8*	*793.1*	*1156.3*	*467.0*	*404.8*
	End of the century	**1064.3**	**1459.1**	**736.7**	**685.1**	**768.5**	**1096.9**	**494.9**	**444.6**
BCCR-BCM2.0	20C3M	1050.9	1492.1	616.3	551.4	825.5	1233.9	446.0	381.2
	Mid of the century	*1145.0*	*1809.5*	*508.2*	*432.8*	*871.4*	*1434.5*	*307.9*	*246.5*
	End of the century	**1145.5**	**1560.6**	**759.3**	**703.6**	**924.1**	**1313.4**	**574.8**	**522.6**
CSIRO-mk3.5	20C3M	1002.2	1490.0	534.7	445.8	786.0	1239.9	379.8	305.9
	Mid of the century	*991.1*	*1449.0*	*533.7*	*457.5*	*791.8*	*1203.5*	*383.4*	*314.6*
	End of the century	**795.3**	**1251.7**	**373.2**	**332.2**	**610.8**	**1031.4**	**242.3**	**205.4**
IPSL-CM4	20C3M	964.0	1363.5	584.2	509.6	744.4	1098.0	412.8	346.6
	Mid of the century	*994.5*	*1438.7*	*582.2*	*535.1*	*777.6*	*1170.2*	*388.4*	*334.4*
	End of the century	**986.4**	**1389.2**	**593.6**	**537.5**	**731.7**	**1097.3**	**401.0**	**343.8**
MPI-ECHAM5	20C3M	1057.3	1517.8	643.8	598.0	838.2	1242.2	461.4	414.3
	Mid of the century	*1087.0*	*1574.9*	*657.4*	*553.9*	*864.3*	*1292.1*	*489.3*	*401.9*
	End of the century	**987.7**	**1392.0**	**587.9**	**546.7**	**749.7**	**1110.8**	**394.9**	**350.9**
Weighted average	20C3M	1026.3	1460.5	622.1	562.8	802.7	1191.4	444.8	385.4
	Mid of the century	*1057.6*	*1546.6*	*601.8*	*527.6*	*822.7*	*1252.1*	*416.7*	*349.2*
	End of the century	**1013.0**	**1424.0**	**633.9**	**584.7**	**767.4**	**1134.2**	**437.9**	**389.6**

* 1) Average annual flow 2) Annual streamflow corresponding to 10% exceedance probability 3) 90% dependable annual flow 4) 95% dependable annual flow 5) Average monsoon flow 6) Monsoon streamflow corresponding to 10% exceedance probability 7) 90% dependable monsoon flow 8)95% dependable monsoon flow.

Table 4
Mann-Whitney test statistics for the percentage change in the mean annual and monsoon flows in the future.

	Mid of the century		End of the century	
	Annual flow	Monsoon flow	Annual flow	Monsoon flow
Test statistic	0.19	0.10	0.10	0.10
Significance level (α)	0.849	0.92	0.92	0.92

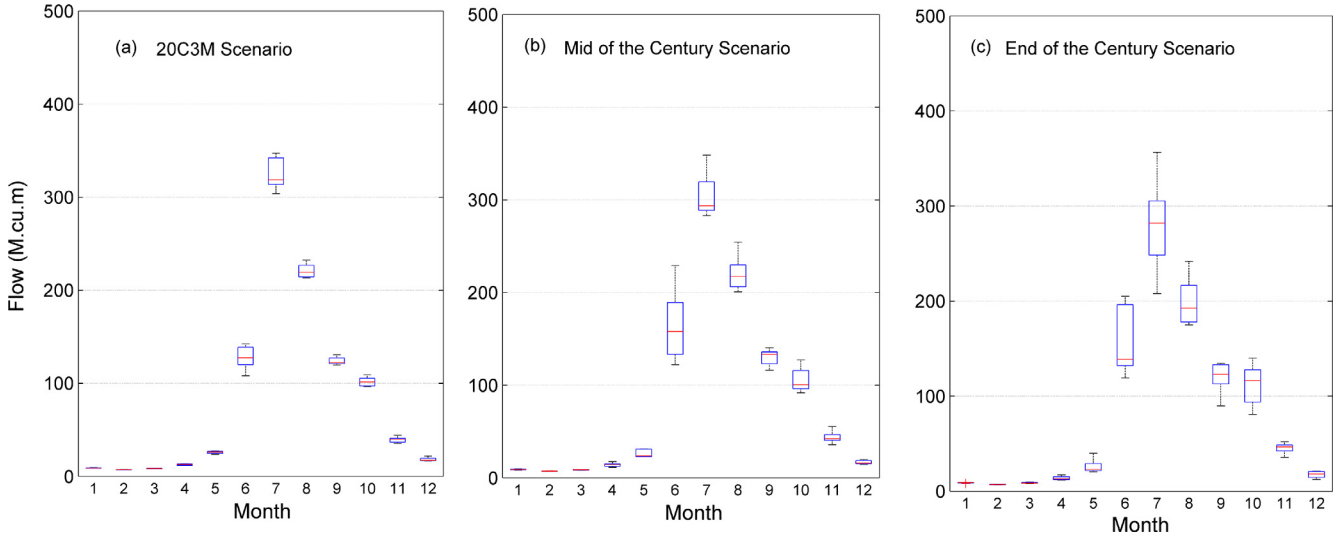

Fig. 6. Comparison of the weighted average monthly flows for the 20C3M scenario and the future time periods. In the box plot, upper and lower hinges represent the 75 and 25 percentiles, respectively. The whiskers show the other data points except the outliers. The line within the box shows the median.

75 percentile flows are projected to increase in June while some reduction is noted during July and August under the future scenario. Close to 25% reduction in the streamflow is observed in July towards the end of the century. Being the peak sowing period for the Kharif crops in India, any drop in the water availability in July in the future scenario may have adverse impact on the agriculture.

4.3. Climate change impact on water budget components

Monthly hydrologic simulations of the catchment under the 20C3M and future scenarios are used to analyse the changes in other catchment water budget components as well. Variations in ET, irrigation demand and groundwater recharge are estimated under the projected climate conditions. Fig. 7 shows the variations

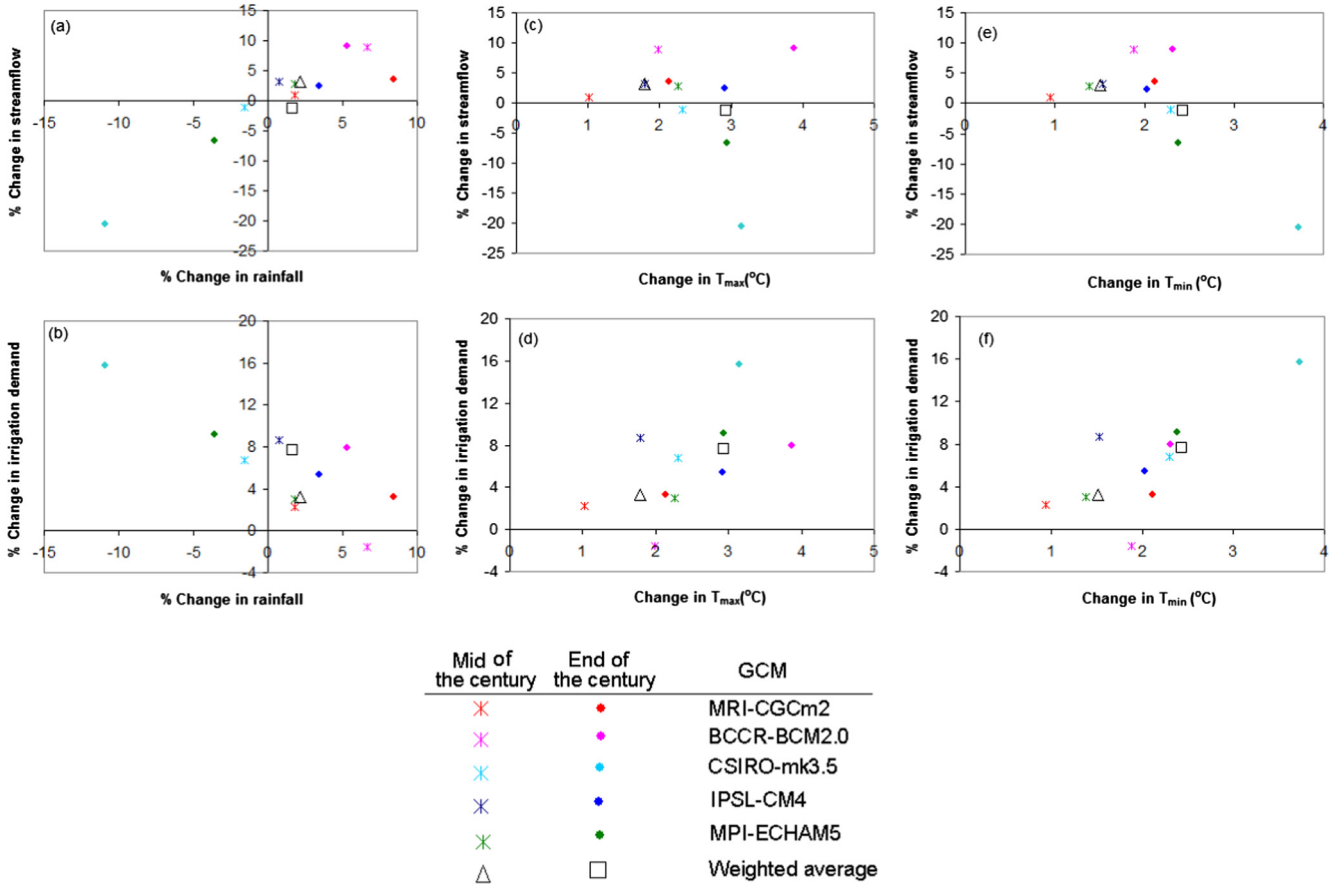

Fig. 7. Relationship between the projected changes in streamflow and irrigation demand with projected changes in the climate from the 5 GCMs.

in streamflow and irrigation demand with the changes in rainfall and temperature. In general, an increase in rainfall causes an increase in streamflow. Rainfall projections from various GCMs vary from −10.9% to 8.4% with respect to the 20C3M scenario, whereas the streamflow projections vary from −20.6% to 9.0% towards the end of the 21st century (Fig. 7a). Likewise, the irrigation demand is projected to increase by 3.2% to 15.7% across various GCMs by the end of the 21st century (Fig. 7b). From Fig. 7a and b it can be observed that changes in the streamflow and irrigation demand are largely related to the variation in rainfall and the GCM. Nevertheless, small deviations may be observed, which may be attributed to the changes in T_{max} and T_{min} as shown in Fig. 7c to f. For example, using BCCR-BCM2.0 larger increases in irrigation demand towards the end of the century is projected, which may be attributed to the highest increase in T_{max} as shown in Fig. 7d. Likewise, results from CSIRO-mk3.5 project significant reduction in streamflow and increase in irrigation demand, which may be attributed to the combined effect of large increases in T_{max} and T_{min}, and significant reduction in rainfall.

Fig. 8 shows the catchment water budget components for the 20C3M scenario at the annual time scale as well as for the monsoon period. Evapotranspiration is the major abstraction from the rainfall amounting close to 70% annually and close to 45% during the monsoon period. Irrigation supplements the crop water demand to a large extent. Ground water recharge is the amount of water that reaches the shallow aquifer. A part of it appears as groundwater flow and contributes to the streamflow at the watershed outlet.

Percentage changes in the water budget components projected under the future scenario with respect to 20C3M scenario at the annual time scale are shown in Fig. 9 a. Weighted ensemble average simulations show marginal increases in annual average rainfall under the future scenarios (2.2% towards the mid of the century and 1.6% towards the end of the century). Though the changes in the annual average rainfall are nominal, the variations in the rainfall pattern in terms of number and durations of wet and dry spells are of major concern. T_{max} is projected to increase by 0.51 °C and 0.84 °C (1.8% and 2.9%) towards the mid of the century and end of the century, respectively. Similarly, T_{min} is projected to increase by 0.29 °C and 0.46 °C (1.5% and 2.4%) towards the mid of the century and end of the century, respectively. With changes in temperature and rainfall pattern, evapotranspiration rates are projected to increase by 2.3% and 4.1%, respectively for the mid of the century and end of the century scenarios. Runoff ratio (ratio of average annual runoff to average annual rainfall) of the catchment is found to be 0.4184, 0.4178 and 0.4083 for 20C3M, mid of the century and end of the century scenarios, respectively. The 2.5% reduction in the runoff ratio shows 1.2% reduction in the annual average streamflow towards the end of the century. In addition, groundwater recharge rates are also projected to decline (by 7.3%) towards the end of the century.

The projected variations in the water budget component may be attributed to the increase in the temperature as well as the changes in the rainfall pattern in the catchment under the future scenarios. The upper catchment is under tropical humid zone, whereas the lower catchment is under semi-arid agro-climatic zone with limited moisture availability. Increase in precipitation and temperature therefore results in increase in evapotranspiration from the catchment and consequently increase in the irrigation demand. Projected increases in the short and moderate

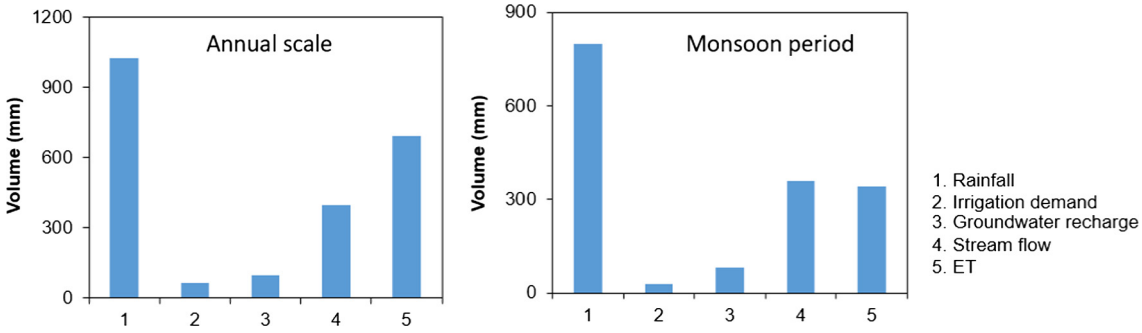

Fig. 8. Water budget components in the Malaprabha catchment for the 20C3M scenario.

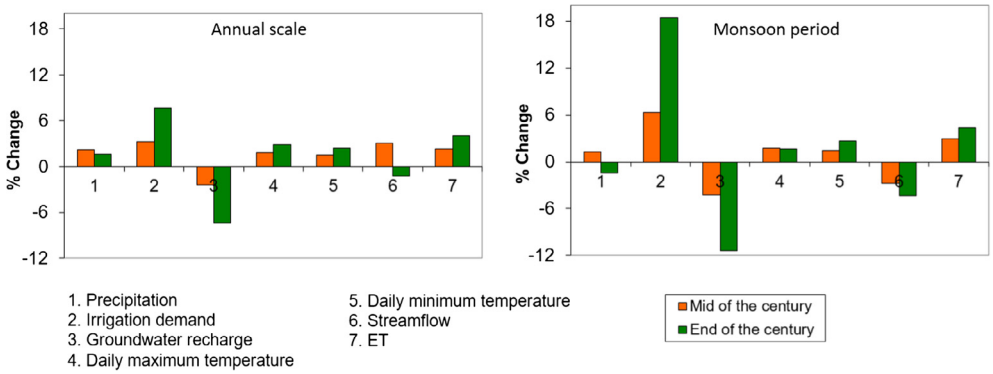

Fig. 9. Percentage changes in the future water budget components with respect to the 20C3M scenario.

rainfall events are likely to cause more infiltration into the soil layer. Thus, a relatively less fraction of rainfall would appear as streamflow at watershed outlet. On the other hand, projected increases in the short and moderate dry spells results in more soil moisture extraction to meet the increased evapotranspiration rates, thereby reducing the groundwater recharge.

Monsoon rainfall being the source of water for the catchment, projected changes in the water budget components during the monsoon season is also studied (Fig. 9 b). During the monsoon period the rainfall is projected to decline by 1.4% towards the end of the century. Reduction in the rainfall together with the increase in the temperature is projected to result in 18.5% increase in the irrigation demand during the monsoon period. In addition, streamflow is also projected to decline under the future scenarios. The analysis shows that percentage changes in the water budget components are more during the monsoon period. This may be attributed to the changes in the rainfall distribution in the form of reduction in the short and moderate wet spells and increase in the dry spells. The projected increase in irrigation demand when combined with the likely reduction in the recharge would aggravate the water scarcity problems of the area, which is already identified as a groundwater overexploited region.

5. Summary and conclusions

This study explores the impacts of climate change on the hydrology and water budget components of the Malaprabha catchment for two future periods (mid of the 21st century, 2046–2065, and end of the century, 2081–2100). In order to address the uncertainty issues that arise from the use of a single GCM, an ensemble of 5 GCMs (MPI-ECHAM5, BCCR-BCM2.0, CSIRO-mk3.5, IPSL-CM4, and MRI-CGCM2) is used in this study. Large scale climate variables simulated by the GCMs are first bias corrected using the NBC approach, and are used to downscale rainfall and meteorological variables at the catchment level using MMM-KDE model. Rainfall and meteorological variables downscaled from each of the 5 GCMs are used as input to a conceptual hydrological model and the corresponding hydrological components for current and future climate scenarios are simulated. Hydrologic simulations using inputs from various GCMs are evaluated for their ability to simulate the hydrologic responses for the 20C3M scenario, and the weights are assigned accordingly. Weighted ensemble average outputs are used to analyse the changes in hydrologic components under the future scenarios. Not many studies have attempted similar kind of work for Indian catchments. The limited data availability and the large scale heterogeneity in the catchment characteristics often hinders such studies. Standing within the constraints of data availability, the study is an efforts to analyse the hydrologic sensitivity of the catchment under the projected climate change scenarios. This would be a stepping stone to understand the climate change vulnerability of the catchment.

The results show only marginal changes in annual average rainfall in the catchment under the future scenarios. Corresponding changes in the hydrologic components are also found to be statistically insignificant both for the annual and monsoon periods. Even though the changes in the streamflow and irrigation demand are strongly related to the variation in rainfall, they are not directly proportional to each other. Such deviations may be attributed to the GCMs used, as well as the changes in rainfall pattern and atmospheric temperature. With 0.84 °C and 0.46 °C increases in the daily maximum and minimum temperatures towards the end of the century, evapotranspiration rate is projected to increase by 4.1%, irrigation demand is projected to increase by 7.7% and groundwater recharge is projected to decline by 7.3%. Streamflow projections for the end of the century scenario show nominal reduction in the average annual and monsoon flows. Changes in

rainfall and temperatures are projected to reduce the runoff ratio by 2.5% by the end of the century. Projected increase in the evapotranspiration and irrigation demand, associated with the decrease in the groundwater recharge and streamflow is an indication of possible aggravation of the water stress in the catchment in future.

Hydrological analyses to investigate the impact of climate change on the catchment water balance are affected by the uncertainty in the climate projections, as well as the uncertainty in the hydrological model itself. In order to reduce the uncertainty in the climate projection, in the present study an ensemble of GCMs included in the CMIP 3 data sets are used to derive the climate projections. On the other hand, uncertainty in the hydrological model still persists. Even though the streamflow simulations are validated with respect to the observed data, lack of sufficient observed data for the catchment restricts the validation of the other water budget components. The use of an ensemble of hydrological models may help to address this issue to some extent. Nevertheless, as reported in literature (Wolock and McCabe, 1999; Arnell and Liv, 2001), the study helps to indicate the sensitivity of the hydrologic systems to the climate change. Analysis using CMIP5 models and representative concentration pathways might help to further understand the impact of climate change projections over the region.

Acknowledgements

This work is supported by the Department of Science and Technology (DST), Government of India under the SERC Fast Track Fellowship Scheme (SR/FTP/ETA-037), Australia India Strategic Research Funds (ST030111 and AISRF-1201628-47) and Ministry of Earth Sciences, Govt. of India (MOES/ATMOS/PP-IX/09). We acknowledge the modeling groups, the Program for Climate Model Diagnosis and Intercomparison (PCMDI) and the WCRP's Working Group on Coupled Modelling (WGCM) for their roles in making available the WCRP CMIP3 multi-model dataset. Support of this dataset is provided by the Office of Science, U.S. Department of Energy. We also express thanks to the Physical Science Division of the NOAA-Earth System Research Laboratory, Boulder, Colorado, USA, for providing the NCEP reanalysis-2 data sets through their website at http://www.esrl.noaa.gov/psd/, and METI and NASA in providing the ASTER GDEM data used in this study.

References

Allen, M.R., Ingram, W.J., 2002. Constraints on future changes in climate and the hydrologic cycle. Nature 419, 224–232. http://dx.doi.org/10.1038/nature01092.

Anandhi, A., Srinivas, V.V., Nanjundiah, R.S., Nagesh Kumar, D., 2008. Downscaling precipitation to river basin in India for IPCC SRES scenarios using Support Vector Machine. Int. J. Climatol. 28, 401–420. http://dx.doi.org/10.1002/joc.1529.

Anandhi, A., Srinivas, V.V., Nagesh Kumar, D., Nanjundia, R.S., 2009. Role of predictors in downscaling surface temperature to river basin in India for IPCC SRES scenarios using support vector machine. Int. J. Climatol. 29, 583–603. http://dx.doi.org/10.1002/joc.1719.

Arnell, N.W., Liv, C., 2001. Hydrology and water resources. In: McCarthy, J.J., Canziani, O.F., Leary, N.A., Dokken, D.J., White, K.S. (Eds.), Climate Change 2001: Impacts. Adaptation and Vulnerability. Cambridge University Press, Cambridge, UK, pp. 191–233.

Arnold, J.G., Srinivasan, R., Muttiah, R.S., Williams, J.R., 1998. Large area hydrologic modeling and assessment- Part I: model development. J. Am. Water Resour. Assoc. 34 (1), 73–89.

Bae, D.H., Jung, I.W., Lettenmaier, D.P., 2011. Hydrologic uncertainties in climate change from IPCC AR4 GCM simulations of the Chungju Basin, Korea. J. Hydrol. 401, 90–105. http://dx.doi.org/10.1016/j.jhydrol.2011.02.012.

Caloiero, T., Coscarelli, R., Ferrari, E., Mancini, M., 2011. Trend detection of annual and seasonal rainfall in Calabria (Southern Italy). Int. J. Climatol. 31 (1), 44–56. http://dx.doi.org/10.1002/joc.2055.

CGWB, 2007. Ground Water Information Booklet, Belgaum District, Karnataka. Central Ground Water Board, Government of India, Bangalore.

Chang, H., Jung, I.W., 2010. Spatial and temporal changes in runoff caused by climate change in a complex large river basin in Oregon. J. Hydrol. 388, 186–207. http://dx.doi.org/10.1016/j.jhydrol.2010.04.040.

Changnon Jr., S.A., 1987. Climate fluctuations and record-high levels of Lake Michigan. Bull. Am. Meteorol. Soc. 68 (11), 1394–1402.

Chen, J., Brissette, F.P., Poulin, A., Leconte, R., 2011. Overall uncertainty study of the hydrological impacts of climate change for a Canadian watershed. Water Resour. Res. 47 (W12509). http://dx.doi.org/10.1029/2011WR010602.

Chen, Y., Takeuchi, K., Xu, C., Chen, Yapeng, Xu, Z., 2006. Regional climate change and its effects on river runoff in the Tarim Basin, China. Hydrol. Process. 20, 2207–2216. http://dx.doi.org/10.1002/hyp.6200.

Dominguez, F., Rivera, E., Lettenmaier, D.P., Castro, C.L., 2012. Changes in winter precipitation extremes for the western United States under a warmer climate as simulated by regional climate models. Geophys. Res. Lett. 39 (L05803). http://dx.doi.org/10.1029/2011GL050762.

Dutta, S., Patel, N.K., Medhavy, T.T., Srivastava, S.K., Mishra, N., Singh, K.R.P., 1998. Wheat crop classification using multidate IRS LISS-I data. J. Indian Soc. Remote Sens. 26 (1–2), 7–14.

Errasti, I., Ezcurra, A., Sáenz, J., Ibarra-Berastegi, G., 2010. Validation of IPCC AR4 models over the Iberian Peninsula. Theoret. Appl. Climatol. 103, 61–79. http://dx.doi.org/10.1007/s00704-010-0282-y.

Ficklin, D.L., Stewart, I.T., Maurer, E.P., 2012. Effects of projected climate change on the hydrology in the Mono Lake Basin, California. Clim. Change 116, 111–131. http://dx.doi.org/10.1007/s10584-012-0566-6.

Fowler, H.J., Blenkinsop, S., Tebaldi, C., 2007. Linking climate change modelling to impacts studies: recent advances in downscaling techniques for hydrological modelling. Int. J. Climatol. 27 (12), 1547–1578.

Frederick, K.D., Major, D.C., 1997. Climatic change and the water resources. Clim. Change 37 (1), 7–23.

Gleckler, P.J., Taylor, K.E., Doutriaux, C., 2008. Performance metrics for climate models. J. Geophys. Res. 113 (D06104). http://dx.doi.org/10.1029/2007JD008972.

Hargreaves, G.H., Samani, Z.A., 1985. Reference crop evapotranspiration from temperature. Trans. ASAE 1 (2), 96–99.

Huntington, T.G., 2006. Evidence for intensification of the global water cycle: review and synthesis. J. Hydrol. 319 (1–4), 83–95.

IPCC, 2013. In: Stocker, T.F., Qin, D., Plattner, G.K., Tignor, M., Allen, K., Boschung, J., Nauels, A., Xia, Y., Bex, V., Midgley, P.M. (Eds.), Climate Change 2013: The Physical Science Basis. Contribution of Working Group I to the Fifth Assessment Report of the Intergovernmental Panel on Climate Change. Cambridge University Press, Cambridge, United Kingdom and New York, NY, USA, p. 1535. http://dx.doi.org/10.1017/CBO9781107415324.

IPCC, SRES, 2000. IPCC Special Report on Emission Scenarios. Cambridge University Press, Cambridge.

Johnson, F., Sharma, A., 2009. Measurement of GCM skill in predicting variables relevant for hydroclimatological assessments. J. Clim. 22, 4373–4382. http://dx.doi.org/10.1175/2009jcli2681.1.

Johnson, F., Sharma, A., 2011. Accounting for interannual variability: a comparison of options for water resources climate change impact assessments. Water Resour. Res. 47 (W04508). http://dx.doi.org/10.1029/2010WR009272.

Johnson, F., Sharma, A., 2012. A nesting model for bias correction of variability at multiple time scales in general circulation model precipitation simulations. Water Resour. Res. 48 (W01504). http://dx.doi.org/10.1029/2011WR010464.

Jung, I.W., Bae, D.H., Lee, B.J., 2012. Possible change in Korean streamflow seasonality based on multi-model climate projections. Hydrol. Process. 27 (7), 1033–1045. http://dx.doi.org/10.1002/hyp.9215.

Kitoh, A., Endo, H., Kumar, K.K., Cavalcanti, I.F.A., Goswami, P., Zhou, T., 2013. Monsoons in a changing world: a regional perspective in a global context. J. Geophys. Res. 118, 3053–3065.

Knutti, R., Furrer, R., Tebaldi, C., Cermak, J., Meehl, G.A., 2010. Challenges in combining projections from multiple climate models. J. Clim. 23, 2739–2758. http://dx.doi.org/10.1175/2009JCLI3361.1.

Lettenmaier, D.P., 1976. Detection of trends in water quality data from records with dependent observations. Water Resour. Res. 12 (5), 1037–1046.

Lillesand, T.M., Kiefer, R.W., Chipman, J.W., 2004. Remote Sensing and Image Interpretation. Wiley India (P) Ltd., New Delhi.

Mann, H.B., Whitney, D.R., 1947. On a test of whether one of two random variables is stochastically larger than the other. Ann. Math. Stat. 18, 50–60.

McCabe, G.J., Wolock, D.M., 2011. Independent effects of temperature and precipitation on modeled runoff in the conterminous United States. Water Resour. Res. 47, W11522. http://dx.doi.org/10.1029/2011WR010630.

McGuffie, K., Henderson-Sellers, A., 1997. A Climate Modeling Primer. John Wiley & sons, West Sussex, England.

Mehrotra, R., Sharma, A., 2010. Development and application of a multisite rainfall stochastic downscaling framework for climate change impact assessment. Water Resour. Res. 46 (W07526). http://dx.doi.org/10.1029/2009WR008423.

Mehrotra, R., Sharma, A., Nagesh Kumar, D., Reshmidevi, T.V., 2013. Assessing future rainfall projections using multiple GCMs and a multi-site stochastic downscaling model. J. Hydrol. 488, 84–100.

Minville, M., Brissette, F., Leconte, R., 2008. Uncertainty of the impact of climate change on the hydrology of a nordic watershed. J. Hydrol. 358 (1–2), 70–83. http://dx.doi.org/10.1016/j.jhydrol.2008.05.033.

Mishra, S.K., Singh, V.P., 2004. Validity and extension of SCS-CN method for computing infiltration and rainfall excess rates. Hydrol. Process. 18, 3323–3345. http://dx.doi.org/10.1002/hyp.1223.

Misra, V., Dirmeyer, P.A., Kirtman, B.P., 2003. Dynamic downscaling of seasonal simulations over South America. J. Clim. 16, 103–117.

Moriasi, D.N., Arnold, J.G., VanLiew, M.W., Bingner, R.L., Harmel, R.D., Veith, T.L., 2007. Model evaluation guidelines for systematic quantification of accuracy in watershed simulations. Trans. ASABE 50 (3), 885–900.

Mueller, B., Seneviratne, S.I., 2014. Systematic land climate and evapotranspiration biases in CMIP5 simulations. Geophys. Res. Lett. 41 (1), 128–134.
Ogata, T., Ueda, H., Inoue, T., Hayasaki, M., Yoshida, A., Watanabe, S., Kira, M., Ooshiro, M., Kumai, A., 2014. Projected future changes of the Asian Monsoon: a comparison of CMIP3 and CMIP5 model results. J. Meteorol. Soc. Jpn. 92, 207–225.
Ojha, R., Nagesh Kumar, D., Sharma, A., Mehrotra, R., 2013. Assessing severe drought and wet events over India in a future climate using a Nested Bias-Correction approach. J. Hydrol. Eng. 18 (7), 760–772.
Oki, T., Kanae, S., 2006. Global hydrological cycles and world water resources. Science 313 (5790), 1068–1072. http://dx.doi.org/10.1126/science.1128845.
Ponce, V.M., Hawkins, R.H., 1996. Runoff curve number: has it reached maturity? J. Hydrol. Eng. 1 (1). http://dx.doi.org/10.1061/(ASCE)1084-0699(1996) 1:1(11).
Reichler, T., Kim, J., 2008. How well do coupled models simulate today's climate? Bull. Am. Meteorol. Soc. 89, 303–311. http://dx.doi.org/10.1175/BAMS-89-3-303.
Reshmidevi, T.V., Jana, R., Eldho, T.I., 2008. Geospatial estimation of soil moisture in rain-fed paddy fields using SCS-CN-based model. Agric. Water Manag. 95 (4), 447–457.
Reshmidevi, T.V., Nagesh Kumar, D., 2012. Modelling the impact of extensive irrigation on the groundwater resources. Hydrol. Process. http://dx.doi.org/10.1002/hyp.9615.
Ruelland, D., Ardoin-Bardin, S., Collet, L., Roucou, P., 2012. Simulating future trends in hydrological regime of a large Sudano-Sahelian catchment under climate change. J. Hydrol. 424–425, 207–216. http://dx.doi.org/10.1016/j.jhydrol.2012.01.002.
Sabeerali, C., Rao, S.A., Dhakate, A., Salunke, K., Goswami, B., 2014. Why ensemble mean projection of south Asian monsoon rainfall by CMIP5 models is not reliable? Clim. Dyn. 45, 1–14.
Saha, A., Ghosh, S., Sahana, A., Rao, E., 2014. Failure of CMIP5 climate models in simulating post-1950 decreasing trend of Indian monsoon. Geophys. Res. Lett. 41, 7323–7330.
Sankarasubramanian, A., Vogel, R.M., 2003. Hydroclimatology of the continental United States. Geophys. Res. Lett. 30 (7), 1363. http://dx.doi.org/10.1029/2002GL015937.
Schaefli, B., Gupta, H.V., 2007. Do Nash values have value? Hydrol. Process. 21 (15), 2075–2080. http://dx.doi.org/10.1002/hyp.6825.
SCS, 1972. National Engineering Handbook, Hydrology Section 4. U.S. Department of Agriculture, Washington D.C..
Sharma, A., Mehrotra, R., Johnson, F., 2012. A new framework for modelling future hydrologic extremes: nested bias correction as a precursor to stochastic rainfall downscaling. In: Surampalli, R.Y., Ojha, C.S.P. (Eds.), Green House Gas Emissions and Climate Change. American Society of Civil Engineers (ASCE), USA.
Shashikanth, K., Salvi, K., Ghosh, S., Rajendran, K., 2014. Do CMIP5 simulations of Indian summer monsoon rainfall differ from those of CMIP3? Atmos. Sci. Lett. 15 (2), 79–85.
Silberstein, R.P., Aryal, S.K., Durrant, J., Pearcey, M., Braccia, M., Charles, S.P., Boniecka, L., Hodgson, G.A., Bari, M.A., Viney, N.R., McFarlane, D.J., 2012. Climate change and runoff in south-western Australia. J. Hydrol. 475, 441–455.
Sooraj, K.P., Terray, P., Mujumdar, M., 2014. Global warming and the weakening of the Asian summer Monsoon circulation: assessments from the CMIP5 models. Clim. Dyn. 45, 1–20.
Sousa, A., García-Murillo, P., Morales, J., García-Barrón, L., 2009. Anthropogenic and natural effects on the coastal lagoons in the southwest of Spain (Doñana National Park). ICES J. Mar. Sci. 66, 1508–1514.
Steenhuis, T.S., Winchell, M., Rossing, J., Zollweg, J.A., Walter, M.F., 1995. SCS runoff equation revisited for variable-source runoff areas. J. Irrig. Drain. Eng. 121 (3). http://dx.doi.org/10.1061/(ASCE)0733-9437(1995) 121:3(234).
Sugawara, M., 1979. Automatic calibration of the tank model. Hydrol. Sci. Bull. 24, 375–388.
Tebaldi, C., Knutti, R., 2007. The use of the multi-model ensemble in probabilistic climate projections. Philos. Trans. R. Soc.: Math., Phys. Eng. Sci. 365 (1857), 2053–2075. http://dx.doi.org/10.1098/rsta.2007.2076.
van Griensven, A., 2005. Sensitivity, auto-calibration, uncertainty and model evaluation in SWAT2005. Unpublished report. http://biomath.ugent.be/~ann/swat_manuals/SWAT2005_manual_sens_cal_unc.pdf (Last accessed 17th December, 2016).
Vaze, J., Teng, J., 2011. Future climate and runoff projections across New South Wales, Australia: results and practical applications. Hydrol. Process. 25, 18–35. http://dx.doi.org/10.1002/hyp.7812.
Wang, S., Kang, S., Zhang, L., Li, F., 2008. Modelling hydrological response to different land-use and climate change scenarios in the Zamu River basin of northwest China. Hydrol. Process. 22, 2502–2510. http://dx.doi.org/10.1002/hyp.6846.
Westerberg, I., Guerrero, J.-L., Seibert, J., Beven, K.J., Halldin, S., 2011. Stage-discharge uncertainty derived with a non-stationary rating curve in the Choluteca River, Honduras. Hydrol. Process. 25, 603–613. http://dx.doi.org/10.1002/hyp.7848.
Wilby, R.L., Harris, I., 2006. A framework for assessing uncertainties in climate change impacts: low-flow scenarios for the River Thames, UK. Water Resour. Res. 42 (W02419). http://dx.doi.org/10.1029/2005WR004065.
Wilcoxon, F., 1945. Individual comparisons by ranking methods. Biometrics 1, 80–83.
Williams, J., 1969. Flood routing with variable travel time or variable storage coefficients. Trans. ASAE 12 (1), 100–103.
Winchell, M., Srinivasan, R., Di Luzio, M., Arnold, J., 2007. ArcSWAT Interface for SWAT2005: User's Guide. Blackland Research Center, Texas Agricultural Experiment Station, Texas and Grassland, Soil and Water Research Laboratory, USDA Agricultural Research Service, Texas.
Woldemeskel, F.M., Sharma, A., Sivakumar, B., Mehrotra, R., 2012. An error estimation method for precipitation and temperature projections for future climates. J. Geophys. Res. 117 (D22104). http://dx.doi.org/10.1029/2012JD018062.
Woldemeskel, F.M., Sharma, A., Sivakumar, B., Mehrotra, R., 2016. Quantification of precipitation and temperature uncertainties simulated by CMIP3 and CMIP5 models. J. Geophys. Res.-Atmos. 121 (1), 3–17.
Wolock, D.M., McCabe, G.J., 1999. Estimates of runoff using water-balance and atmospheric general circulation models. J. Am. Water Resour. Assoc. 35 (6), 1341–1350.
Xu, Z.X., Takeuchi, K., Ishidaira, H., 2003. Monotonic trend and step changes in Japanese precipitation. J. Hydrol. 279 (1–4), 144–150. http://dx.doi.org/10.1016/S0022-1694(03)00178-1.
Yu, P.S., Yang, T.C., 2000. Using synthetic flow duration curves for rainfall-runoff model calibration at ungauged sites. Hydrol. Process. 14, 117–133.
Zhang, H., Huang, G.H., 2013. Development of climate change projections for small watersheds using multi-model ensemble simulation and stochastic weather generation. Clim. Dyn. 40, 805–821. http://dx.doi.org/10.1007/s00382-012-1490-1.